Supplementary Electronic Material

S1. Experimental

Additional experiments investigating the interaction of CO with argon, krypton, methane, ethane and dihydrogen sulfide were also performed, and are reported in this additional supplementary material. These interactions have much less (or indeed no) relevance to the interstellar spectroscopy, but are useful in identifying and understanding the trends in the spectroscopic behaviour of CO. Argon (99.999%, BOC), krypton (99.999%, BOC), ethane (99.95%, Messer Griesheim), and dihydrogen sulfide (99.6%, BDH) were used without further purification. Methane was studied using computational methods only. The first cooling stage of the cryostat is inconveniently at the desorption temperature of methane, causing slow desorption following methane deposition, and preventing ultrahigh vacuum from being obtained. The experimental methods used are as described in section 2 of the main text. The computational methods used are as described in section 3 of the main text, with the exception that the 3-21G basis set was applied to Kr.

S2. Results

The spectra ν_{CO} band for CO interacting with Ar, Kr, C_2H_6 and H_2S surfaces, and sandwiched in within these species, are shown in Fig. S1. Peak positions and widths are summarised in Table S1. The CO interaction with each species is discussed in turn below. The configurations of the stable complexes as determined by the *ab initio* calculations are shown in Figs. S2 – S6, and the energetic, spectroscopic and bond length data corresponding to these complexes are displayed in Table S2. Comparisons of the experimental results with gas phase and matrix isolation experiments from the literature are made in Table S3.

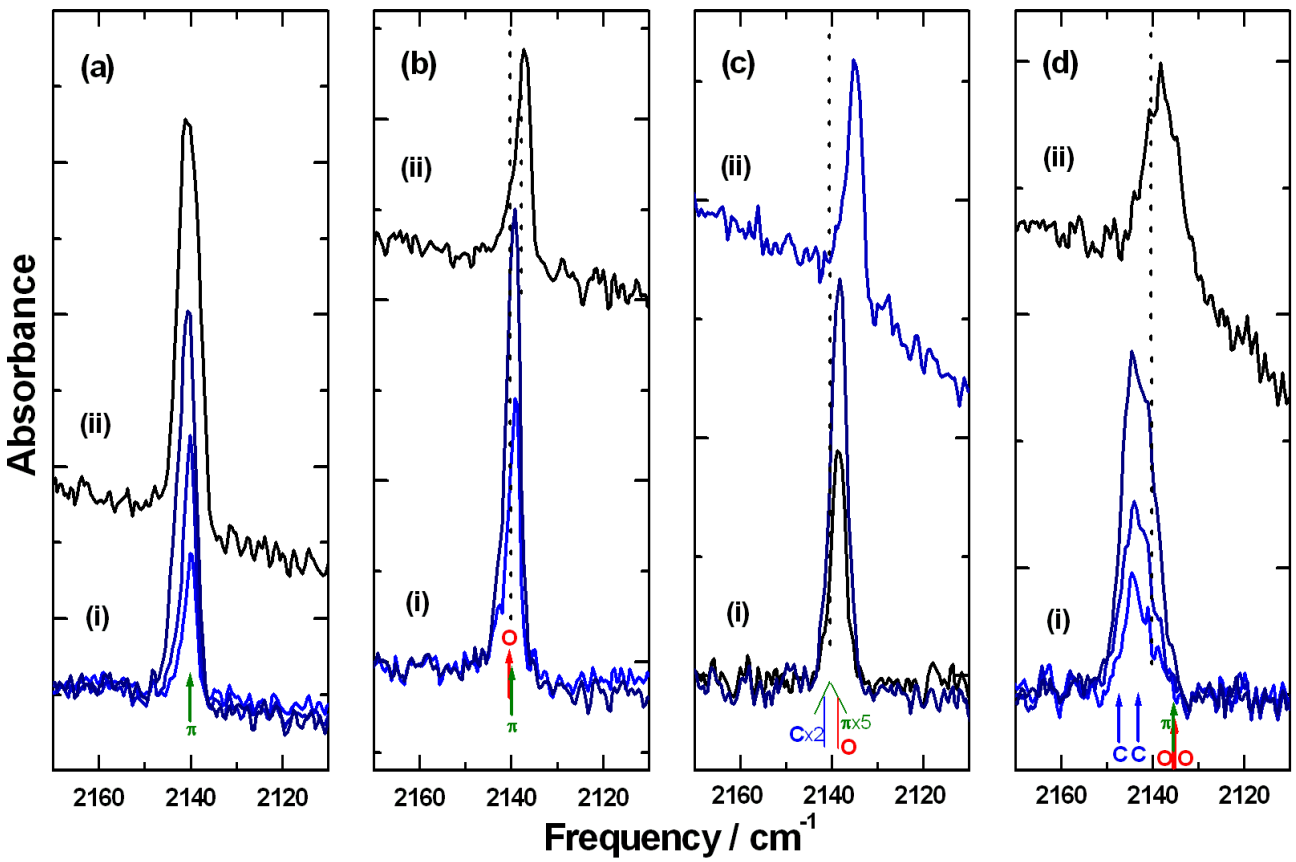

Fig. S1 RAIR difference spectra of CO adsorbed on **(a)** argon; **(b),** krypton; **(c),** C_2H_6 and **(d)** H_2S**; (i)** 0.25 L ((a) and (d) only), 0.50 L and 1.0 L of CO adsorbed at 8 K onto a 50 L film of the second species pre-deposited at 8 K, **(ii)** 1.0 L CO ((a) and (d)) or 0.5 L CO ((b) and (c)) 'sandwiched' at 8 K between 50 L deposits of the second species; spectra of the initially deposited 50 L film have been subtracted in each case. Arrows mark the predicted frequencies of ν_{CO} vibrations of C_{CO}-bonded, O_{CO}-bonded and π-bonded molecules for stable CO complexes in the *ab initio* calculations. The dotted line marks the position of the ν_{CO} vibration for CO adsorbed on an argon surface.

Table S1 ν_{CO} peak positions and widths for 0.5 L of CO adsorbed on, and 1.0 L CO sandwiched in films of various species.

Film Species	Peak Position {FWHM} / cm^{-1}	Shift[a]	Sandwich Peak Position {FWHM} / cm^{-1}	Shift[b]
Ar	2140.1 {3.2}	0.0	2140.4 {6.0}	0.0
Kr	2139.6 {3.1}	–0.5	2137.4 {3.7}[c]	–3.0
C_2H_6	2138.7 {4.0}	–1.4	2135.2 {3.8}[c]	–5.2
H_2S	2143.4 {5.7} ~2140	3.3 ~ 0	2138.1 {8.4}	–2.3

[a] relative to ν_{CO} for the gas phase Ar/CO at 2140.1 cm^{-1}.

[b] relative to ν_{CO} for CO sandwiched between argon layers at 2140.4 cm^{-1}.

[c] data for 0.5 L CO sandwiched.

S2.1 CO-Ar Interaction

The ν_{CO} peak for the 0.25 L CO exposure on Ar is 2140.1 cm^{-1}, and is relatively narrow (Fig. S1a(i)). As the coverage increases, the peak broadens slightly, and is shifted to higher frequency by less than 1 cm^{-1}, reflecting the increase in CO-CO interactions. The ν_{CO} peak in the sandwiched film at 2140.4 cm^{-1} is slightly broader still (Fig. 1a(ii)).

The CO-Ar complex is well known, and one of the most thoroughly studied van der Waals complexes, both experimentally and theoretically [S1-S6]. Spectroscopic investigations of the gas phase CO-Ar complex in the infrared [S1] and microwave [S2] have established that its geometry is close to 'T' shaped, with the O atom slightly closer to the Ar atom. The origin of the ν_{CO} frequency for the CO-Ar complex has been experimentally observed to be red shifted by 0.44 cm^{-1} with respect to that of the CO monomer [54]. In recent years, the computational studies have produced models with consistent results [S3-S6]. The predicted stabilities fall within the 1.2 to 1.3 kJ mol^{-1} range, with 'T' shaped geometries tilted toward either the C or O atoms by no more than 5°. Our *ab initio* calculations reproduce this geometry (Fig. S2), and predict a ν_{CO} frequency shift close to that experimentally measured However, the stability is much lower than previously reported, and in fact after BSSE correction, the predicted complex is unstable. As with the CO dimer, the matrix isolation of CO in argon has been extensively studied, with varying peak positions and assignments given [28,29,69]. Abe *et al.* [69] report two ν_{CO} peaks, at 2138.5 cm^{-1} and 2136.7 cm^{-1} attributed to librating and non-librating CO monomers, respectively.

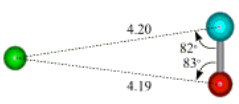

Fig. S2 Local minimum geometry for the predicted CO-Ar complex. Marked bond distances are in angstroms.

S2.2 CO-Kr Interaction

The ν_{CO} stretch feature of the CO on Kr system shows a red shift of 0.5 cm^{-1}, and is somewhat narrower than for CO on other surfaces (Fig. S1b(i)). The peak is red shifted by 3.0 cm^{-1} in the sandwich experiment, and although broader than for CO adsorbed on the Kr surface, it remains much narrower than for the sandwich experiments for other systems (Fig. S1b(ii)).

The gas phase CO-Kr complex has been studied experimentally in supersonic free jet expansions using infrared [S7,S8], microwave [S9] and millimetre wave [S10] spectroscopy. The origin of the ν_{CO} band is shifted by 0.63 cm^{-1} with respect to the CO monomer [S8], and a 'T' shaped structure determined [S9]. *Ab initio* computational studies of the CO-Kr complex using coupled-cluster theory have found it to be stabilised by 1.43 kJ mol^{-1}, and to have a 'T' shaped structure with the CO···Kr bond tilted by roughly 9° with the C atom closer to the Kr atom [S11,S12]. Our *ab initio* calculations produced a slightly more tilted geometry (Fig. S3(i)), in addition to a linear C-bonded complex (Fig. S3(ii)). Again, the predicted stabilities of these complexes are much lower than the previously calculated value, and become negative after BSSE correction, although the ν_{CO} frequency shift of the 'T' shaped structure reproduces the experimental observation well. The infrared spectrum of CO isolated in krypton matrix has also been previously studied [S13,S14]. As in argon, peaks for librating and non-librating CO molecules were identified, with red shifts of 2.8 and 3.8 cm^{-1}, respectively [S14].

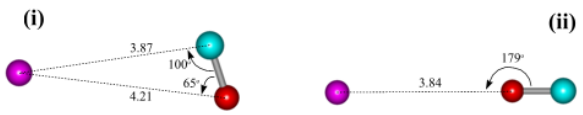

Fig. S3 Local minimum geometry for the predicted CO-Kr complexes. Marked bond distances are in angstroms.

S2.3 CO-C_2H_6 Interaction

The RAIR spectrum of the 50 L initially deposited C_2H_6 film (not shown) is in reasonable agreement with previously published IR spectra [S15]. It is consistent with the formation of an amorphous film, as is expected from previous IR and Raman studies [S16,S17]. The ν_{CO} band for CO adsorbed on C_2H_6 is red shifted by 1.4 cm^{-1} (Fig. S1c(i)). A more substantial red shift of 5.2 cm^{-1} is observed for CO sandwiched in C_2H_6, although the peak is slightly less broad than that of CO adsorbed on the C_2H_6 surface.

Eight weakly bound complexes were identified in our *ab initio* calculations (Fig. S4(i)-(viii)), although following vibrational analysis, five of these structures appear to be saddle point geometries. A linear O≡C···H–CH_2CH_3 complex (Fig. S4(i)) is the most stable of the complexes, although following BSSE correction this, and all seven other, structures were found to have negative binding energy.

We have not located any publications that study the CO-C_2H_6 complex, either experimentally or theoretically. Furthermore, we know of no infrared studies of co-deposited CO and ethane in the literature. However, Schriver *et al.* report the frequency of the ν_{CO} band for CO reactively formed by UV photolysis of CO_2-C_2H_6 mixtures to be 2140 cm^{-1} [S15], although this region of the spectrum is not shown in detail and the precision of this frequency is not known.

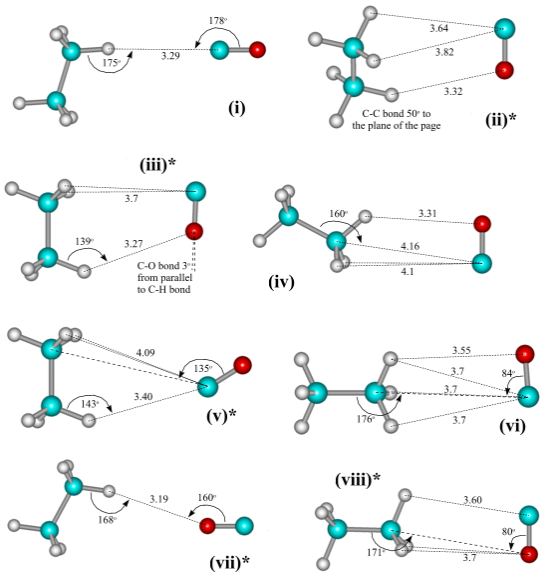

Fig. S4 Local minimum geometry for the predicted CO-C_2H_6 complexes. Marked bond distances are in angstroms. Complexes found to be saddle point geometries based on vibrational analysis are marked *.

S2.4 CO-CH_4 Interaction

Given the lack of published data with which to compare the RAIR spectra and *ab initio* calculations for the CO-C_2H_6 system, it is worth considering previous studies of the interaction between CO and methane. We were not able to study this system experimentally – the temperature of the heat shield on our cryostat coincides with the desorption temperature of methane, meaning that UHV can not be attained after deposition of methane. Studies of the gas phase CO-CH_4 complex have demonstrated that the origin of the ν_{CO} band is red shifted by 0.63 cm^{-1} with respect to the CO monomer [S18], and that its geometry to be essentially 'T' shaped [S19]. To our knowledge, the CO-CH_4 complex has not been studied within the matrix of a rare gas, however, the infrared spectrum of CO within a CH_4 matrix has been recorded [S20]. A ν_{CO} peak lies at about the frequency expected for matrix isolated CO. Two additional peaks with significant blue and red shifts were observed, although no interpretation of the spectra was offered. A red shifted ν_{CO} peak was also observed in an equimolar co-deposition of CO and CH_4 [S21]. This was supported by *ab initio* calculations of the gas phase CO-CH_4 complex at second order Møller-Plesset perturbation level of theory (MP2), which found two nearly isoenergetic structures, with tilted linear O–C···H–CH_3 and C–O···H–CH_3 geometries and high stabilities of around 14 kJ mol^{-1}. Both structures were found to have substantially red shifted ν_{CO} frequencies.

Our *ab initio* calculations found three weakly bound structures: a linear O≡C···H–CH_3 complex, a linear C≡O···H–CH_3 complex and a tilted 'T'-shaped complex which is similar to the experimentally determined geometry of the gas phase complex (Figs. S5(i)-(iii)). However, the latter two structures were found to be saddle point geometries. Only the linear C≡O···H–CH_3 complex was stable following BSSE correction. The predicted ν_{CO} frequencies showed a slight blue shift for the linear O≡C···H–CH_3 complex and slight red shifts for the tilted 'T'-shaped and linear C≡O···H–CH_3 complexes.

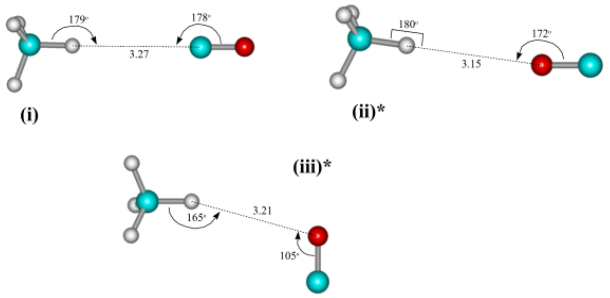

Fig. S5 Local minimum geometry for the predicted CO-CH_4 complexes. Marked bond distances are in angstroms. Complexes found to be saddle point geometries based on vibrational analysis are marked *.

S2.5 CO-H_2S Interaction

The RAIR spectrum obtained for the initially deposited H_2S film (not shown) displayed good agreement with the bands identified in a previously published transmission IR study [S22], and confirms that the deposited film adopted an amorphous structure, rather than any of the three crystalline structures previously identified [S23,S24]. For a 0.25 L exposure of CO on H_2S the ν_{CO} band is centred with a blue shift of 3.3 cm^{-1}, although it is non-symmetrical and the peak maximum is a further 0.7 cm higher in frequency (Fig. 1d(i)). As the CO exposure is increased to 1.0 L, the peak broadens and the asymmetry increases, giving the strong suggestion of a second contribution to the peak at a red shift of roughly 1 cm^{-1}. The ν_{CO} band for CO sandwiched between H_2S films shows a 2.0 cm^{-1} red shift (Fig. 1d(ii)).

Infrared spectroscopy of the gas phase CO-H_2S complex has measured the origin of the ν_{CO} band to be blue shifted by 3.8 cm^{-1} with respect to the CO monomer [S25], although no geometry has been reported. Computational studies of the complex using MM [S26] and MP2 *ab initio* [S27] methods found the same two stable geometries, both linearly aligned with the S–H bond, and interacting via either the C or O atom. However, the HS–H···OC complex was found to be the global minimum geometry with a stability of 3.67 kJ mol^{-1} in the MM study [S26], whereas in the MP2 study, the HS–H···CO complex was substantially more stable, with a stability of 5.22 kJ mol^{-1} [S26]. The shifts in the ν_{CO} frequency were also calculated in the MP2 study, with a red shift of 2.7 cm^{-1} predicted for the C≡O···H–SH complex and a larger blue shift of 5.2 cm^{-1} predicted for the O≡C···H–SH complex [S27]. These were compared to observed vibrational features for the CO-H_2S complex formed by photolytic decomposition of monothioformic acid in an argon matrix [S27]. A broad feature centred at 2143 cm^{-1} was attributed to the CO-H_2S complex, although the authors speculated that interconversion between various geometries may induce the breadth of the peak, since the barrier to conversion has been calculated to be very low [S26].

Our *ab initio* calculations identified five stable geometries for the isomer, all of which were planar. The linear O≡C···H–SH complex (Fig. S6(i)) was the most stable after geometry optimisation, but following BSSE correction the linear C≡O···H–SH complex (Fig. S6(ii)) was found to be the global minimum, with a stability of 1.29 kJ mol^{-1}. The latter was also the most frequently obtained geometry. The other geometries were a tilted compact structure with a H···O interaction (Fig. S6(iii)), a H···C 'elbow' complex (Fig. S6(iv)) and a bifurcated H_2···O 'arrow' complex (Fig. S6(v)) in which the O≡C bond points at the S atom from between the two hydrogen atoms, although vibrational analysis suggests that this fifth complex is a saddle point geometry. The predicted ν_{CO} frequencies were blue shifted from that of the CO monomer by 6.93 cm^{-1} and 2.82 cm^{-1} for the linear O≡C···H–SH and C···H 'elbow' complexes, respectively, and red shifted by 5.69 cm^{-1}, 5.46 cm^{-1} and 5.24 cm^{-1} for the linear C≡O···H–SH, compact O≡C‖H–SH and 'arrow' complexes, respectively.

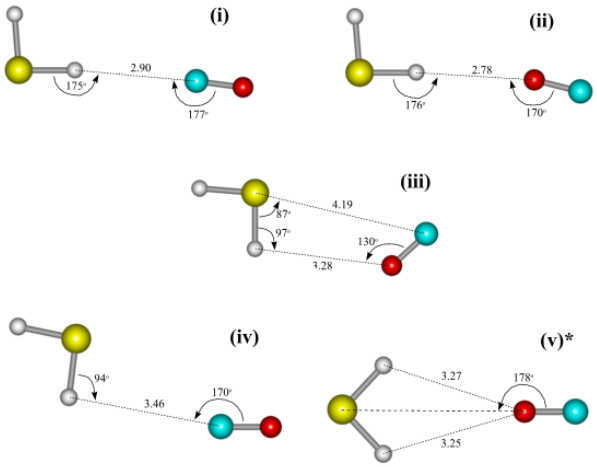

Fig. S6 Local minimum geometry for the predicted H_2S···CO complexes. Marked bond distances are in angstroms. Complexes found to be saddle point geometries based on vibrational analysis are marked *.

Table S2. A summary of results of *ab initio* calculations for complexes of CO with various species.

Complex	CO Bonding Configuration	Starting Geometries Optimised [a]	Uncorrected Stability / kJ mol^{-1}	Corrected Stability / kJ mol^{-1}	C≡O Bond Length / Å	Corrected (Surface) ν_{CO} / cm^{-1} [b]	Corrected (Gas Phase) ν_{CO} / cm^{-1} [c]
CO monomer		**1**	-----	-----	1.11365	-----	2143.27
CO-Ar Fig. S2		3					
'T' shaped	π	1	0.132	-0.170	1.11367	2140.1	2142.75
CO-Kr Fig. S3		**3**					
'T'-shaped; (i)	π	1	0.822	-0.783	1.11367	2140.0	2142.70
C≡O···Kr linear; (ii)	O_{CO}	1	0.532	-0.759	1.11364	2140.5	2143.16
CO-C_2H_6 Fig. S4		**12**					
O≡C···H–CH_2CH_3 linear; (i)	C_{CO}	1	0.834	-0.282	1.11350	2141.7	2144.38
H_2···C≡O···H bridged; (ii)*	π	4	0.767	-0.317	1.11382	2139.7	2142.31
C≡O‖H_3C–CH_3 parallel; (iii)*	π	1	0.765	-0.278	1.11381	2138.6	2141.28
O≡C‖H–CH_2CH_3 planar; (iv)	π	1	0.680	-0.192	1.11356	2139.5	2142.17
O≡C┤H_3C–CH_3 'T'-shaped; (v)*	C_{CO}	1	0.652	-0.298	1.11356	2140.7	2143.39
O≡C‖H–CH_2CH_3 non-planar; (vi)	π	2	0.604	-0.201	1.11372	2139.7	2142.35
C≡O···H–CH_2CH_3 linear; (vii)*	O_{CO}	1	0.521	-0.061	1.11373	2140.1	2142.78
C≡O‖H–CH_2CH_3 parallel; (viii)*	π	1	0.515	-0.207	1.11365	2140.2	2142.30
CO-CH_4 Fig. S5		**10**					
O≡C···H–CH_3 linear; (i)	C_{CO}	3	0.918	-0.200	1.11348	2142.0	2144.66
C≡O···H–CH_3 linear; (ii)*	O_{CO}	1	0.606	0.005	1.11373	2139.4	2141.07
CO├H–CH_3 'T'-shaped; (iii)*	π	5	0.691	-0.159	1.11385	2138.9	2142.55
CO-H_2S Fig. S6		**20**					
O≡C···H–SH linear; (i)	C_{CO}	3	2.423	0.744	1.11279	2147.5	2150.20
C≡O···H–SH linear; (ii)	O_{CO}	9	2.057	1.292	1.11427	2134.9	2137.58
O≡C‖H–SH compact; (iii)	π	5	2.043	0.926	1.11427	2135.2	2137.81
O≡C···H–SH elbow; (iv)	C_{CO}	1	2.034	0.709	1.11327	2143.4	2146.09
C≡O···H_2S arrow; (v)*	O_{CO}	2	1.647	1.101	1.11425	2135.4	2138.03

* saddle point geometries.

[a] Where the sum of the optimisations for individual complexes does not equal the total number of optimisations for that system then some starting geometries optimise dto a non-bonding configuration.

[b] raw frequencies are scaled by a factor of 0.87666.

[c] raw frequencies are scaled by a factor of 0.87776.

Table S3 A summary of the shifts in ν_{CO} due to interaction of CO with other species for gas phase complexes, matrix isolated complexes and surface adsorption.

Interaction	Gas Phase [a]	Matrix Isolation [b]	Surface Adsorption [c]
CO-Ar	0	0, –1.8 [d, 69]	0
CO-Kr	–0.19 [S8]	–2.8, –3.8 [e, S14]	–0.7
CO-C_2H_6	-----	1.5 [f, S15]	-----
CO-CH_4	–0.19 [S18]	6.0, –2.9 [g, S20]	–0.8
CO-H_2S	4.2 [S25]	4.5 [S27]	3.3, ~0

[a] relative to ν_{CO} for the gas phase CO-Ar complex at 2142.83 cm^{-1} [54].
[b] value for the CO complex in an argon matrix relative to ν_{CO} for a librating CO monomer in an argon matrix at 2138.5 cm^{-1} [69].
[c] relative to ν_{CO} of CO on an argon film at 2140.6 cm^{-1}; this work.
[d] values for the librating and non-librating CO monomers, respectively.
[e] values for the librating and non-librating CO monomers, respectively, in a krypton matrix.
[f] value for CO in an ethane matrix.
[g] values for CO in a methane matrix.

S3. Discussion

The five additional systems analysed in this supplementary material provide broad support for the conclusions of the main paper (and indeed were part of the data set used to reach these conclusions). The interactions of CO with the Ar, Kr, and C_2H_6 and CH_4, are very weak, and the shifts in ν_{CO} frequency, both experimentally measured and computationally predicted, are small, and thus it is difficult to make any specific comments about the interactions in these systems. The interactions predicted for the CO-H_2S complexes are stronger, and the shifts in ν_{CO} frequency are more significant. The moderately blue shifted ν_{CO} frequency of the gas phase CO-H_2S complex is consistent with a C_{CO}-hydrogen bonded complex, although the geometry was not determined [S25]. There is computational support for such a complex from both our own and previously published studies, although this geometry is not clearly favoured over the O_{CO}-hydrogen bonded complex. Matrix isolation data also supports a C_{CO}-bonded complex, although allows for multiple configurations For CO adsorbed on the H_2S surface, the observation of a blue shifted peak consistent with CO molecules bonded *via* the C_{CO} atom, with π interacting molecules contributing to a possible unshifted component. In contrast to other systems showing a blue shifted surface adsorption, the shift is less than that in the gas phase complex. This may reflect the weaker hydrogen bonding interactions in the H_2S film in comparison amorphous H_2O.

Supplementary References

S1 A. R. W. McKellar, Y. P. Zeng, S. W. Sharpe, C. Wittig, R. A. Beaudet, *J. Mol. Spectrosc.*, 1992, **153**, 475.
S2 T. Ogata, W. Jäger, I. Ozier, M. C. L. Gerry, *J. Chem. Phys.*, 1993, **98**, 9399.
S3 R. R. Toczyłowski, S. M. Cybulski, *J. Chem. Phys.*, 2000, **112**, 4604, and references therein.
S4 F. A. Gianturco, F. Paesani, *J. Chem. Phys.*, 2001, **115**, 249.
S5 T. B. Pedersen, J. L. Cacheiro, B. Fernandez, H. Koch, *J. Chem. Phys.*, 2002, **117**, 6562.
S6 L. H. Coudert, I. Pak, L Surin, *J. Chem. Phys.*, 2004, **121**, 4691, and references therein.
S7 M. D. Brookes, A. R. W. Walker, *Mol. Phys.*, 1999, **97**, 127.
S8 A. R. W. McKellar, *J. Mol. Spectrosc.*, 1993, **158**,100.
S9 K. A. Walker, T. Ogata, W. Jäger, M. C. L. Gerry, I. Ozier, *J. Chem. Phys.*, 1997, **106**, 7519.
S10 K. A. Walker, A. R. W. Walker, *J. Mol. Spectrosc.*, 2001, **205**, 331.
S11 E. Feng, Z. Wang, M. Gong, Z. Chi, *J. Chem. Phys.*, 2007, **127**, 174301.
S12 Z. Wang, M. Gong, Y. Zhang, E. Feng, Z.Cui, *Chem. Phys. Lett.*, 2008, **458**, 7.
S13 H. Dubost, *Chem. Phys.*, 1976, **12**, 139.
S14 H. Abe, K. M. T. Yamada, *Struct. Chem.*, 2003, **14**, 211.
S15 A. Schriver, L. Schriver-Mazzuoli, P. Ehrenfreund, L. d'Hendecourt, *Chem. Phys.*, 2007, **334**, 128.
S16 M. G. Wisnosky, D. F. Eggers, L. R. Fredrickson, J. C. Decius, *J. Chem. Phys.*, 1983, **79**, 3505.
S17 M. G. Wisnosky, D. F. Eggers, L. R. Fredrickson, J. C. Decius, *J. Chem. Phys.*, 1983, **79**, 3513.
S18 C. Xia, K. A. Walker, A. R. W. Walker, *J. Chem. Phys.*, 2001, **114**, 4824.
S19 Y. Liu, W. Jäger, *J. Chem. Phys.*, 2004, **121**, 6240.
S20 A. G. Maki, *J. Chem. Phys.*, 1961, **35**,931.
S21 W. Z. Alsindi, D. O. Gardner, E. F. van Disheock, H. J. Fraser, *Chem. Phys. Lett.*, 2003, **378**, 178.
S22 K. Fathe, J. S. Holt, S. P. Oxley, C. J. Pursell, *J. Phys. Chem. A* 110, (2006) 10793.
S23 F. P. Reding, D. F. Hornig, *J. Chem. Phys.*, 1957, **27**, 1024.
S24 W. Zheng, R. I . Kaiser, *Chem. Phys. Lett.*, 2007, **440**, 229.
S25 C. Xia, A. R. W. McKellar, *J. Molec. Spec.*, 2005, **229**, 39.
S26 G. de Oliveira, C. E. Dykstra, *J. Mol. Struct.: THEOCHEM*, 1996, **362**, 235.
S27 J. Lundell, E. Nordquist, M. Räsänen, *J. Molec. Struct.*, 1997, **416**, 235.